

CONTROLLER DESIGN FOR ACTIVE CLOSED-LOOP CONTROL OF CAVITY FLOWS

P. Yan¹, M. Debiasi², X. Yuan¹, E. Caraballo², M. Ö. Efe^{1,5}, H. Özbay^{1,§}, M. Samimy²,
J. DeBonis³, R. C. Camphouse⁴, J. H. Myatt⁴, A. Serrani¹, J. Malone²

*Collaborative Center for Control Science
The Ohio State University*

¹Department of Electrical Engineering, The Ohio State University, Columbus, OH 43210

²Department of Mechanical Engineering, The Ohio State University, Columbus, OH 43210

³NASA Glenn Research Center, Brookpark, OH 44135

⁴Air Force Research Laboratory, Air Vehicles Directorate, WPAFB, OH 45433

⁵Now with the Department of Mechatronics Engineering, Atılım University, Ankara, Turkey

[§] Corresponding author: part the work was done at Bilkent Univ., Dept. of Electrical and Electronics Eng., Ankara, Turkey, e-mail: ozbay@ee.eng.ohio-state.edu, hitay@bilkent.edu.tr

Abstract

In this paper we discuss feedback controller design issues for active control of shallow cavity flows. Linear controllers, such as H^∞ , PID, and Smith predictor based controllers are designed and tested experimentally. The ineffectiveness of using fixed linear models in the design of linear controllers for the cavity flows is demonstrated via experimental results. In order to better address this problem, we are in the process of developing a nonlinear model of the cavity flow dynamics using Proper Orthogonal Decomposition (POD). We briefly discuss control issues related to the class of feedback systems involving this type of nonlinear plants.

1. Introduction

Active closed-loop control of cavity flow has been chosen as a benchmark problem by the flow control group of the Collaborative Center of Control Science (CCCS) at The Ohio State University. A general overview of the research activities of this group appears in Samimy et al. (2003a, 2003b) and in a companion paper (Samimy et al. 2004). Although flow-induced cavity resonance is a well-studied problem (see Cattafesta et al. 2003 for a recent review), the effects of the closed loop dynamic control on the flow dynamics are not well understood yet. Therefore, feedback controller design for active closed loop cavity flow control is still an open problem.

The difficulty in the controller design lies in the fact that the flow dynamics are governed by the Navier-Stokes equations, which, in control terminology, are infinite dimensional and highly nonlinear. These equations cannot be solved sufficiently fast for any practical models, and hence they cannot be used in any “internal model control” scheme. Recently, a physics based linear model was proposed and used in control of

cavity oscillations (Rowley et al. 2002). As a first step, we used a similar type of linear model for controller design and tested it experimentally. The linear controllers designed are deliberately chosen to be relatively simple (PID controller, Smith predictor-based controller, and H^∞ controller) so that stability analysis can be done easily, solely based on the linear feedback theory. The experimental results summarized in Section 4 do not match the expected results from the linear feedback theory. Whereas the open loop (in the absence of external forcing) system response of the linear model to a white noise fits the experimental data very well. Thus, we conclude that a nonlinear input-output model should be used for feedback controller design. However, this model should be simple enough for analysis of the effect of feedback control.

Therefore, as the next step, we try to develop a reduced order nonlinear model, which captures the essential dynamics of the flow due to external forcing. This model is based on the Proper Orthogonal Decomposition (POD) and Galerkin projections (see Caraballo et al. 2003; Samimy et al. 2003b & 2004). Similar approaches to modeling cavity flows are also

being considered by others (e.g. Rowley et al. 2000, 2003). In this paper, we touch upon the characteristics of this low order nonlinear model from a system theory point of view.

The linear model is described in Section 2, and the controllers designed for this model are given in Section 3. The corresponding experimental results can be found in Section 4. The input-state-output form of the low order nonlinear model is given in Section 5, and concluding remarks are made in Section 6. The overall activity of the group, including details of the experimental work, can be found in our companion paper (Samimy et al. 2004).

2. Physics Based Linear Model of the Cavity Flow

The physics-based linear model introduced in Williams et al. (2002) and Rowley et al. (2002) involve separate linear transfer function blocks for the shear layer, $G(s)$, scattering, K_S , acoustic feedback, and receptivity, K_R , as shown in Figure 2.1. The plant transfer function contains two internal feedbacks: acoustic feedback, and receptivity. The shear layer can be taken to be a second order system with a time delay:

$$G(s) = \frac{\omega_0^2 e^{-s\tau_s}}{s^2 + 2\zeta\omega_0 s + \omega_0^2}, \quad (2.1)$$

where the parameters are determined from the experimental data. If we define the acoustic feedback as

$$A(s) = \frac{e^{-s\tau_a}}{1 - r(s)e^{-2s\tau_a}} \quad (2.2)$$

$$r(s) = \frac{r}{1 + s/\omega_r}$$

and model the receptivity feedback and scattering as constant gains. Then, the plant transfer function becomes

$$P(s) = \frac{K_S G(s) A(s)}{1 - K_R K_S G(s) A(s)}. \quad (2.3)$$

The parameters of the above linear system can be optimized to match the open loop response of the cavity pressure fluctuations, at a given fixed Mach number. That is, when the feedback controller is taken out of the loop, the output power spectrum matches the power spectrum of the pressure fluctuations measured at the center bottom of the cavity. Figure 2.2 illustrates this observation. The parameters of the plant that generate the response shown in this figure are listed below, where unity gains are for actuator and sensor dynamics, see Yuan et al. (2003). For these specific parameter values the plant is stable.

| | |
|------------|-------------|
| ω_0 | 200 rad/sec |
| ζ | 0.95 |
| τ_s | 0.0195 sec |
| τ_a | 0.001 sec |
| r | 0.1 |
| ω_r | 100 rad/sec |
| K_R | 0.408 |
| K_S | 1.65 |
| K_v | 1 |
| K_m | 1 |

3. Linear Controllers Based on the Linear Model

3.1 H^∞ Controller Design

The H^∞ controllers are primarily designed to reduce the effect of the uncertainty on the system response, Doyle et al. (1992). In our particular case, for the cavity flow control, we can define a sensitivity minimization problem to compare the open loop and closed loop responses. The open loop system response is

$$|P(j\omega)| \quad (3.1)$$

and the closed loop response is

$$\frac{|P(j\omega)|}{|1 + P(j\omega)C(j\omega)|} \quad (3.2)$$

so we would like to minimize the weighted sensitivity over all stabilizing controllers, the weight being the plant itself. Similar techniques from linear robust control theory have been used for cavity flow control in Rowley and Williams (2003). They have discussed the effects of actuator saturation too, using describing function analysis.

We note that for the numerical values given above the plant is stable and can be written in the form

$$\begin{aligned} P(s) &= N_{o1}(s)N_{o2}(s)M_n(s) \\ N_{o2}(s) &= K_S G_0(s) = \frac{K_S}{1 + 2\zeta s/\omega_0 + s^2/\omega_0^2} \\ M_n(s) &= e^{-h_1 s} \quad h_1 = \tau_s + \tau_a \\ N_{o1}(s) &= (1 - K_R N_{o2}(s)M_n(s) - r(s)M_2(s))^{-1} \\ M_2(s) &= e^{-2\tau_a s} \end{aligned} \quad (3.3)$$

Since the plant and the weight are infinite dimensional, there is no direct and easy solution to this weighted sensitivity minimization problem. For the case where the plant, or the weight, is finite dimensional the problem can be solved using certain results from operator theory, Foias et al. (1996). In this particular case, we approximate the weight by another infinite dimensional transfer function, which captures the essential dynamics within a large frequency region,

and then by exploiting this special structure we solve the problem, see Yuan et al. (2003) for details. The controller is in the form given below:

$$C(s) = C_2(s) (1 - r(s)M_2(s)) + K_R \quad (3.4)$$

where

$$C_2(s) = \left(\frac{\gamma}{\gamma_{\min}} - \frac{\gamma_{\min}}{\gamma} \right) \frac{N_{o2}(s)^{-1}}{(1 + as + bs^2)} \left(\frac{1}{1 + H(s)} \right) \quad (3.5)$$

and

$$H(s) = H_{\text{FIR}}(s) + H_{\text{IIR}}(s). \quad (3.6)$$

These FIR and IIR filters, as well as all the other parameters (including γ , γ_{\min} , a , and b) appearing in the above formula, can be explicitly computed, Yuan et al. (2003). Note that the controller is infinite dimensional, but it can be implemented using finite dimensional terms, delay blocks, and an FIR filter. In fact, controller complexity did not pose any severe restrictions when we implemented it on dSPACE real-time control boards (see Section 4).

The simulation result shown in Figure 3.1 illustrates that when the plant is taken to be the linear model defined above, then the H^∞ controller is able to suppress the strong sinusoidal oscillations seen at the output.

3.2 Smith Predictor Design

Smith predictors are simple controllers typically used for plants represented by a second order transfer function with a time delay, like $G(s)$ defined above. In this case, the controller structure is as shown in Figure 3.2, where C_0 is a stabilizing controller for the delay free part, G_0 , such that the delay-free closed loop system

$$\frac{G_0(s)}{1 + G_0(s)C_0(s)} \quad (3.7)$$

is stable. Then, the closed loop feedback response from noise to the output becomes the delayed version of the above closed-loop transfer function, which is designed just from the delay-free part of the plant. This idea is used for the delayed second-order transfer function representation of the cavity flow system. For C_0 we took a simple first order controller placing the poles as far left in the complex plane as possible.

3.3 PID Controller Design

The classical PID controller has three terms, proportional, integral and derivative:

$$C(s) = K_p + \frac{K_i}{s} + \frac{K_d s}{\varepsilon s + 1} \quad (3.8)$$

Besides the gains of these three terms, a small parameter ε is introduced for causality of the controller. There are several tuning techniques for the PID gains for linear plants. But in the actual experimental set-up we first used a proportional (P) controller only, and searched for its best gain by trial and error. We have noticed that adding an integral term does not change the system behavior. We believe that this is due to the fact that the actuator is not able to generate very low frequency signals (and also recall that the actual system is nonlinear, so linear design rules do not always work here – more on this in Section 4). Similarly the derivative term did not have a significant impact on this system. The experimental results on all of the above controllers are given in the next section.

4. Experimental Results

In this section we summarize the experimental results observed for the controllers designed above. For the details of the experimental set-up we refer to Debiasi and Samimy (2003), and also to our companion paper Samimy et al. (2004). It suffices here to recall that pressure fluctuations were measured by a Kulite XTL-190-25A dynamic pressure transducer mounted on the cavity floor. A dSPACE 1103 controller board connected to a Dell Precision Workstation 650 computer was used to acquire at 50 kHz through a 12 bit channel the Kulite signal that was then manipulated to produce the desired control signal from a 14 bit output channel. In order to maximize the control board performance, its processor was used exclusively for running the control routines. Simultaneous data were recorded by the computer at a sampling frequency of 200 kHz through a National Instruments 6036E 16 bit DAQ board.

Debiasi and Samimy (2003) introduced a search method for an optimal sinusoidal input frequency at any given Mach number. This scheme has been studied further in Samimy et al. (2004) to better understand the coupling effect of the input with the natural Rossiter modes. The experimentally observed resonant frequencies at different Mach numbers are compared to the Rossiter frequencies predicted analytically in Figure 4.1, see also the companion paper, Samimy et al. (2004). In this work we choose the Mach number 0.3 as our baseline uncontrolled case. The Sound Pressure Level (SPL) derived from the recorded data is shown in Figure 4.2 from which we see that the power is concentrated in the 3rd Rossiter mode at the frequency of about 2800 Hz.

First, we designed a PID controller by simply searching for the best controller parameters by manually adjusting them. It turned out that, due to the actuator dynamics, the integral term does not have any

significant effect on the system response since the loudspeaker cannot produce very low frequency signals, where integral action is most significant. Similarly, the derivative term did not have a significant impact; so we replaced it with a first order filter with an adjustable cut-off frequency to have a PD-like controller in the form

$$C(s) = K_p + K_d \frac{\tau_d s}{\tau_d s + 1} e^{-hs} \quad (4.1)$$

Note that when $h=0$ and τ_d is small we have the derivative action, with appropriate scaling of K_d . Otherwise, when τ_d is large, the system behaves like a P-P controller (two proportional terms), which is equivalent to a single proportional term, but later we will add a non-zero time delay, h , to introduce zeros. This is the reason why we keep the two terms separate when τ_d is large.

The second type of controller has the Smith predictor form, as discussed in Section 3.2, and it is based on a second order transfer function with a time delay fit to the baseline case.

The H^∞ controller is derived as outlined in Section 3.1 for the linear model of the baseline case, whose structure is as given in Section 2.

These three controllers, designed for $M=0.3$, were tested in the experimental facility for $M=0.27$ and $M=0.3$. The results are very similar in all three cases as illustrated in Figures 4.3, 4.4, and 4.5. All these controllers are successful in eliminating (or significantly reducing) the main frequency of oscillation (third Rossiter mode), but they lead to strong oscillations with frequency about 1900 Hz in the vicinity of the second Rossiter mode. This is expected since the linear controllers were designed for the baseline case and thus excitement of the other Rossiter modes was not taken into account. Therefore, the controllers should be re-designed in such a way that the second Rossiter mode does not get excited. With this observation in mind we turned our attention to the simple PD-like controller, whose optimal parameters were found to be:

$$K_p = 8, \quad K_d = 0.04, \quad \tau_d = 200.$$

By adding a time delay of $h=260 \mu s$ to the “derivative” term we put a 180 degree phase shift for signals operating at 1923Hz, i.e. in the neighborhood of the second Rossiter frequency. The performance of this PD-like controller with delay on the Mach 0.27 and 0.3 flows is shown in Figure 4.6. It is interesting to note that the performance of this controller was also quite satisfactory at Mach numbers with multi-mode resonance (as shown in Fig. 4.6 (c) for Mach 0.37) or at higher Mach numbers exhibiting stronger, single-mode resonance at the 2nd Rossiter mode (as shown in Fig. 4.6

(d) for Mach 0.43). Since τ_d is relatively large, the controller acts like a P-P control with individual delay terms. In fact, we changed the controller to

$$C(s) = 8(1 + e^{-hs}), \quad h = 260 \mu s \quad (4.2)$$

in order to place a “zero” in the frequency response exactly at 1923Hz. We noticed that the performance of this controller is very much like the performance of the PD-like controller with the same time delay.

5. Nonlinear Models of the Cavity Flow

The experimental results showed us that when we derive a linear model from the baseline experiments (without external forcing input) the model does not contain any information on other Rossiter modes, which could potentially get excited in the flow. Linear controllers derived from such a linear model do not perform well, in the sense that they are likely to excite one or more of the other modes. This observation has been made previously in the literature; see e.g. Cattafesta et al. (2003) and their references. In order to avoid this situation, a better nonlinear model is sought. We have been working in this line in parallel, Caraballo et al. (2003), Samimy et al. (2003b). The approach taken is the POD based low order nonlinear modeling, as in Berkooz et al. (1993), Freund and Colonius (2002), and many others. Next, we summarize the latest results in this line of work, taken from our companion paper Samimy et al. (2004), and then discuss control theoretic issues associated with this model. We also discuss extensions of the POD-based nonlinear model, and other nonlinear models.

5.1 Structure of the POD-based Nonlinear Model

The main goal of the POD-based low dimensional modeling work is to characterize the flow in the cavity in terms of certain orthogonal basis functions, and their time coefficients. For example, in the 2-D case, we would like to be able to write the stream-wise velocity $u(t,x,y)$, at any time instant t and any point (x,y) in the cavity, as

$$u(t, x, y) \approx \sum_{k=1}^N \alpha_k(t) \varphi_k(x, y) \quad (5.1)$$

where spatial modes, φ_k , are fixed, and they are determined from the simulation data, and time coefficients, α_k , satisfy an N^{th} order ordinary differential equation, see Caraballo et al. (2003) and Samimy et al. (2003b) for details of how this is done. As illustrated in Samimy et al. (2004), the N^{th} order ODE that the temporal variables satisfy can be written in a compact input to state equation form, and moreover the pressure output is shown to be a linear combination

of the time coefficients. Thus, we deal with a nonlinear system, whose dynamics are in the form

$$\begin{aligned} \dot{\alpha}(t) &= A_0 + A_1 \alpha(t) + \begin{bmatrix} \alpha^T(t) A_{21} \alpha(t) \\ \vdots \\ \alpha^T(t) A_{2n} \alpha(t) \end{bmatrix} + (B_1 + \begin{bmatrix} \alpha^T(t) B_{21} \\ \vdots \\ \alpha^T(t) B_{2n} \end{bmatrix}) \Gamma(t) \\ p(t) &= M \alpha(t) \end{aligned} \quad (5.2)$$

$\alpha(t)$: vector of time coefficients

$\Gamma(t)$: input voltage applied to the actuator

$p(t)$: pressure output signal

and all the matrices involved in the above equation can be considered to be dependent only on the Mach number. In fact we have observed that they vary slightly depending on the input signal applied, but this dependence is very difficult to express analytically and it is not as significant as the dependence on the Mach number.

Therefore, for a given fixed Mach number, we will try to design a feedback controller for the above nonlinear system.

5.2 Control Problems Associated with the POD-based Nonlinear Model

One of the first tasks we are facing now is the implementation of the nonlinear dynamical system model described in Section 5.1, with feedback controller in the loop (see Figure 5.1), in Matlab's Simulink environment. Then, we will compare its results under the same feedback control schemes defined in Section 4. Once we verify that these simulation results match the above-mentioned experimental results, we can safely assume that the nonlinear model captures the essential dynamical behavior of the system under different feedback control schemes.

The next task, then, will be controller design for the above nonlinear input-state-output model. There are several system theoretic issues to be addressed, specifically:

- Is there a limit cycle around an equilibrium state?
- What is the fundamental frequency of the limit cycle?
- How does the input affect the magnitude and frequency of oscillations?
- How do the model parameters change with the Mach number?

5.3 Interpolation of POD-based Nonlinear Models

A fundamental issue in the POD based flow modeling is the validity range of the model. It is known that the dynamical content of the model depends upon

the snapshots of the flow, which constitute the sole source of information for the POD model. This way of thinking stipulates the following fact: dynamical richness of a POD model is characterized by the snapshots. Conversely, a POD model cannot synthesize a behavior whose signature is absent in the snapshots. This results in a locality problem, which can be addressed by the use of fuzzy decision mechanisms. The use of such an expert soft-switching approach would allow us to switch between different POD models that are valid for different operating conditions. An example of this approach is shown on 1-D Burgers equation with successful results in Efe et al. (2004a).

5.4 Modeling by Neural Networks

Neural networks are well known for their powerful nonlinear mapping capabilities. The computational flexibility and the diversity of algorithms allowing the designer to tune for a given map makes neurocomputing a good technique for flow modeling and control, Haykin (1994), Jang et al. (1997). Such applications are involved with the imprecision in the measured quantities, nonlinear process dynamics, presence of multiple and potentially nonlinear subsystems and so on. A combination of these in a single application limits the applicability of pure mathematical techniques and encourages the use of computationally feasible and high performance devices such as neural systems. Technically speaking, given some history of the inputs (excitation or control signal) and outputs (pressure readings from some particular locations of the cavity), a neural network can be trained such that the output at the next time instant is estimated.

We have used the data collected from the experimental setup to train such a neural network, as shown in Figure 5.2, with the settings given below. Note that to keep the notation consistent with the literature on neural networks we have defined the voltage input applied at discrete time instant k as $u(k)$, the observed pressure output $d(k)$, and the estimated pressure output $x(k)$.

- The neural identifier has the structure 5-12-1
- Hidden neurons have hyperbolic tangent nonlinearity
- Output neuron is linear
- Inputs are $[x(k) \ x(k-1) \ u(k) \ u(k-1) \ u(k-2)]$, and the output is $x(k+1)$
- One epoche is the feedforward pass of 16,381 data pairs
- Training takes 188 epoches ($\approx 1/2$ hour time on a P4 PC)
- Mean squared error decreases to 8.85e-6
- The data is collected at 200 kHz sampling rate
- Training algorithm is the Levenberg-Marquardt technique.

For training the network, we have used the data collected for the excitation input given by zero mean 4 V_{rms} amplitude sine wave at 2 kHz. Successively, we have tested the trained network against the data collected for the excitation input of a zero mean 4 V_{rms} amplitude sine wave at 3.25 kHz. Figure 5.3, which is taken from Efe et al. (2004b), shows the comparison of the frequency contents of the measured and estimated pressure output signals. For time domain simulation results, and details of the neural network map we refer to Efe et al. (2004b).

6. Concluding Remarks

The long-term goal of our project is to derive new design techniques for closed loop aerodynamic flow control. As a first step, we have chosen cavity flow as the benchmark problem, and tried simple linear controllers, designed from linear models that match the open loop response of the system very well. Our experimental results confirmed previously observed phenomena: (i) linear controllers derived from a single dominant mode plant model are able to suppress the cavity oscillations at this frequency, but they shift the oscillations to another Rossiter frequency, which was not visible in the unforced case but could easily be excited; (ii) adding a zero to the controller at this hidden Rossiter frequency avoids this problem.

By using extensive simulations, we derived a nonlinear model based on the POD. Next, we will test this nonlinear model under linear feedback by using Matlab/Simulink based simulations. Then, by exploiting the structure of this type of nonlinear systems, we will derive nonlinear controllers, to be tested experimentally. Our previous studies have shown that POD-based models are dependent not only on the Mach number, but also on the frequency of external input signal. Interpolation of the local models will also be studied, as well as neural network based models.

Acknowledgements

This work is supported in part by the AFRL/VA and AFOSR through the Collaborative Center of Control Science (Contract F33615-01-2-3154) and by DAGSI. The simulation work is supported in part under NASA Glenn's Aerospace Propulsion and Power Base Research and Technology Program and in part by a grant of computer time from the DOD High Performance Computing Modernization Program at the Army Research Laboratory.

References

Berkooz, G., Holmes, P., and Lumley, J. L., "The Proper Orthogonal Decomposition in the Analysis of

Turbulent Flows," *Annual Review of Fluid Mechanics*, Vol. 25, 1993, pp. 539-575.

Caraballo, E., Samimy, M., and DeBonis, J., "Low Dimensional Modeling of Flow for Closed-Loop Flow Control," AIAA Paper 2003-0059, January 2003.

Cattafesta, L. N. III, Williams, D. R., Rowley, C. W., and Alvi, F. S., "Review of Active Control of Flow-Induced Cavity Resonance," AIAA Paper 2003-3567, June 2003.

Debiasi, M., and Samimy, M., "An Experimental Study of the Cavity Flow for Closed-Loop Flow Control," AIAA Paper 2003-4003, June 2003.

Doyle J. C., Francis, B. A., and Tannenbaum, A. R., *Feedback Control Theory*, Macmillan Publishing Co., 1992.

Efe, M. Ö., Yuan, X., Özbay, H., and Samimy, M., "Interpolating the Local Models of POD Using Fuzzy Decision Mechanisms," submitted to 9th Mechatronics Forum, Ankara, Turkey, August-September 2004a.

Efe, M. Ö., Debiasi, M., Özbay, H., and Samimy, M., "Modeling of Subsonic Cavity Flows by Neural Networks," submitted to Int. Conf. on Mechatronics (ICM'04), Istanbul, Turkey, June 2004b.

Foias, C., Özbay, H., and Tannenbaum, A. R., *Robust control of infinite dimensional systems: Frequency domain methods*, LNCIS, No.209, Springer-Verlag, Berlin, 1996.

Freund, J. B., and Colonius, T., "POD Analysis of Sound Generation by a Turbulent Jet," AIAA Paper 2002-0072, January 2002.

Haykin, S., (1994). *Neural Networks*, Macmillan College Printing Co., New Jersey, 1994.

Jang, J.-S. R., Sun, C.-T., and Mizutani, E., *Neuro-Fuzzy and Soft Computing*, Prentice-Hall, New Jersey, 1997.

Kegerise, M. A., Cattafesta, L. N. III, and Ha, C.-S., "Adaptive Identification and Control of Flow-Induced Cavity Oscillations," AIAA Paper 2002-3158, June 2002.

Rowley, C. W., Colonius, T., and Murray, R. M., "Dynamical Models for Control of Cavity Oscillations," AIAA Paper 2001-2126, May 2001.

Rowley, C. W., Williams, D. R., Colonius, T., Murray, R. M., MacMartin, D. G., and Fabris, D., "Model-Based Control of Cavity Oscillations Part II: System Identification and Analysis," AIAA Paper 2002-0972, January 2002.

Rowley, C. W., and Williams, D.R., "Control of Forced and Self-Sustained Oscillations in the Flow past a Cavity," AIAA Paper 2003-0008, January 2003.

Samimy, M., Debiasi, M., Caraballo, E., Malone, J., Little, J., Özbay, H., Efe, M. Ö., Yan, P., Yuan, X., DeBonis, J., Myatt, J. H., and Camphouse, R. C., "Exploring Strategies for Closed-Loop Cavity Flow Control," AIAA Paper 2004-0576, January 2004.

- Samimy, M., Debiasi, M., Caraballo, E., Özbay, H., Efe, M. Ö., Yuan, X., DeBonis, J., and Myatt, J. H., "Closed-Loop Active Flow Control – A Collaborative Approach," AIAA Paper 2003-0058, January 2003a.
- Samimy, M., Debiasi, M., Caraballo, E., Özbay, H., Efe, M. Ö., Yuan, X., DeBonis, J., and Myatt, J. H., "Development of Closed-Loop Control for Cavity Flows," AIAA Paper 2003-4258, June 2003b.
- Williams D. R., Rowley, C. W., Colonius, T., Murray, R. M., MacMartin, D. G., Fabris, D., and Albertson, J., "Model Based Control of Cavity Oscillations Part I: Experiments," AIAA Paper 2002-0971, January 2002.
- Yuan, X., Efe, M. Ö., and Özbay, H., "On Delay-Based Linear Models and Robust Control of Cavity Flows," *NSF-CNRS Workshop on Time Delay Systems*, Paris, France, January 2003.

Figures

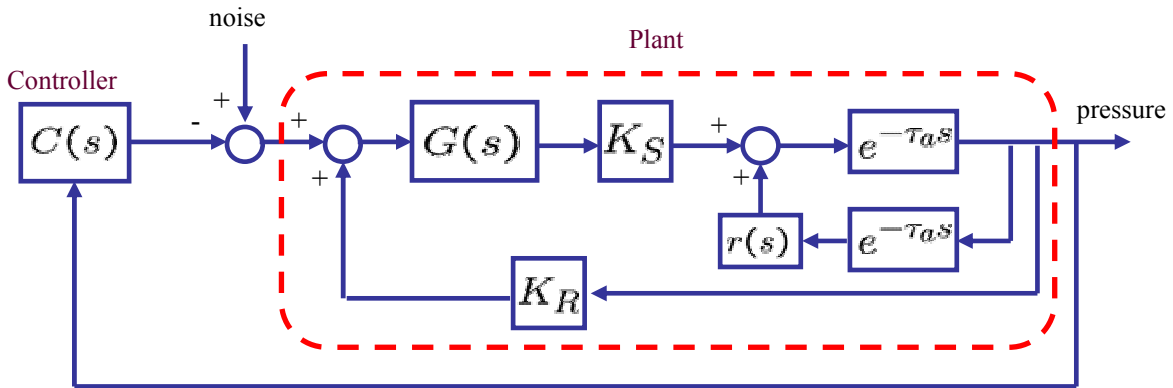


Figure 2.1 Linear feedback system.

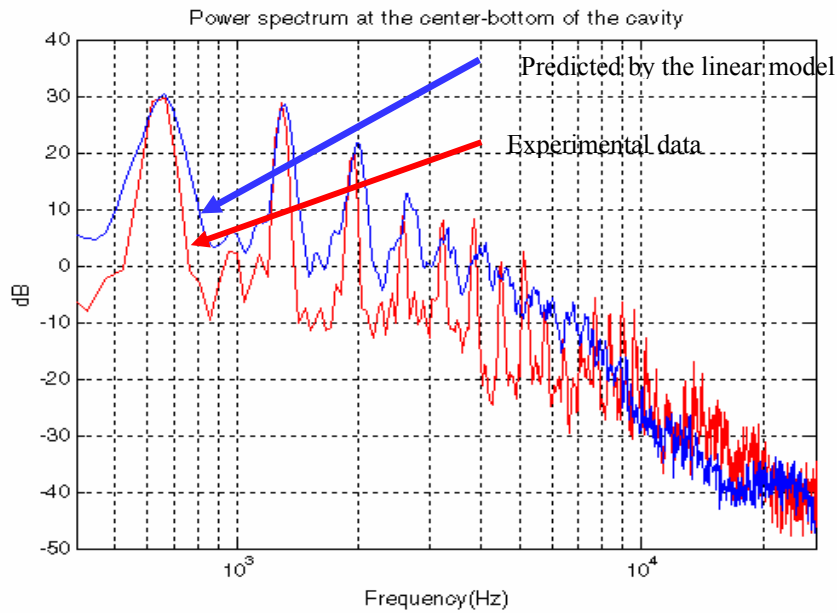


Figure 2.2 Comparison of output power spectra from experimental data and the linear model.

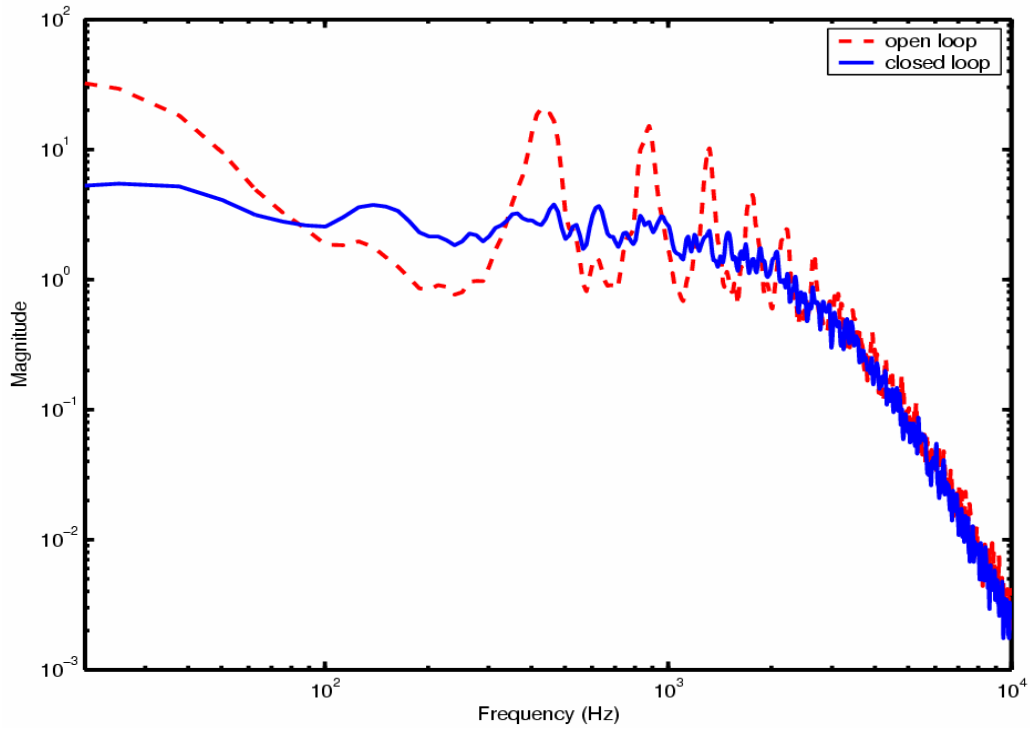


Figure 3.1. H^∞ controller performance for the plant described by the linear model.

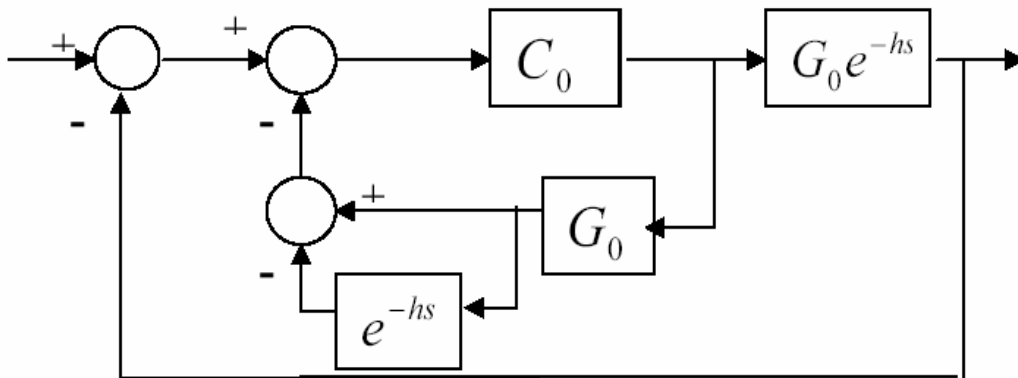


Figure 3.2 Structure of the Smith predictor controller

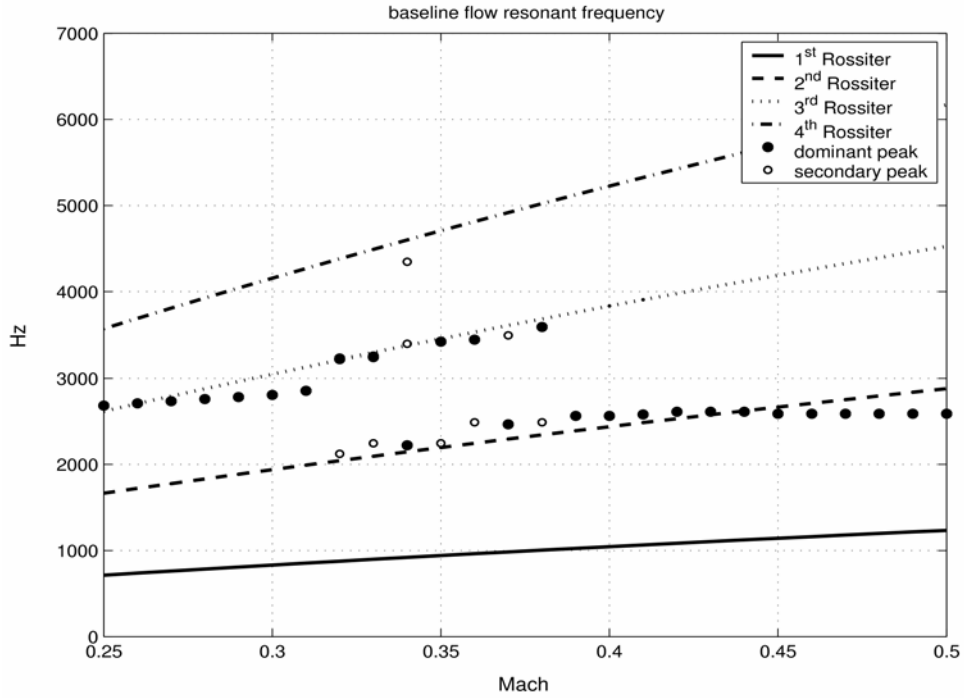


Figure 4.1 Rossiter frequencies (lines) and measured frequencies (circles) as a function of the flow Mach number.

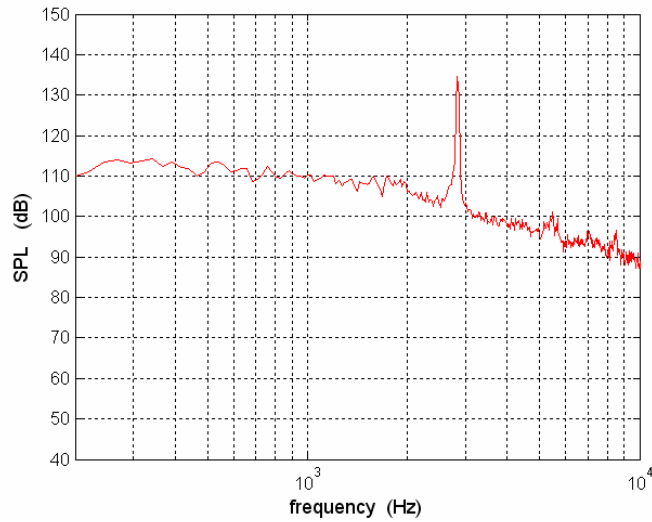


Figure 4.2 Cavity-flow SPL spectrum at the center of the cavity floor for the baseline case (no control) M=0.3 flow.

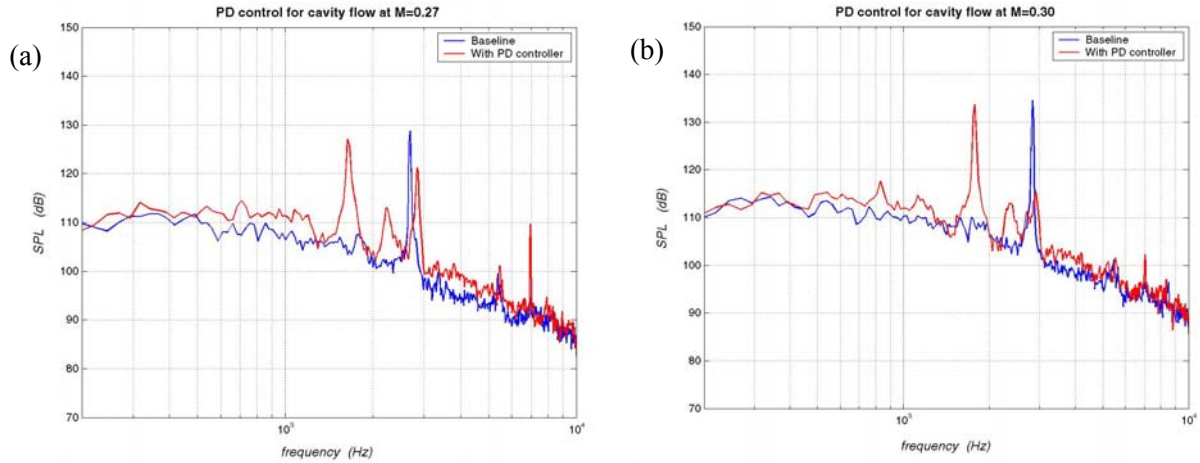


Figure 4.3 Effect of PD control on Mach 0.27 flow (a) and on Mach 0.3 flow (b); upper (thin) line is the baseline flow SPL spectrum and lower (thick) line is the controlled flow.

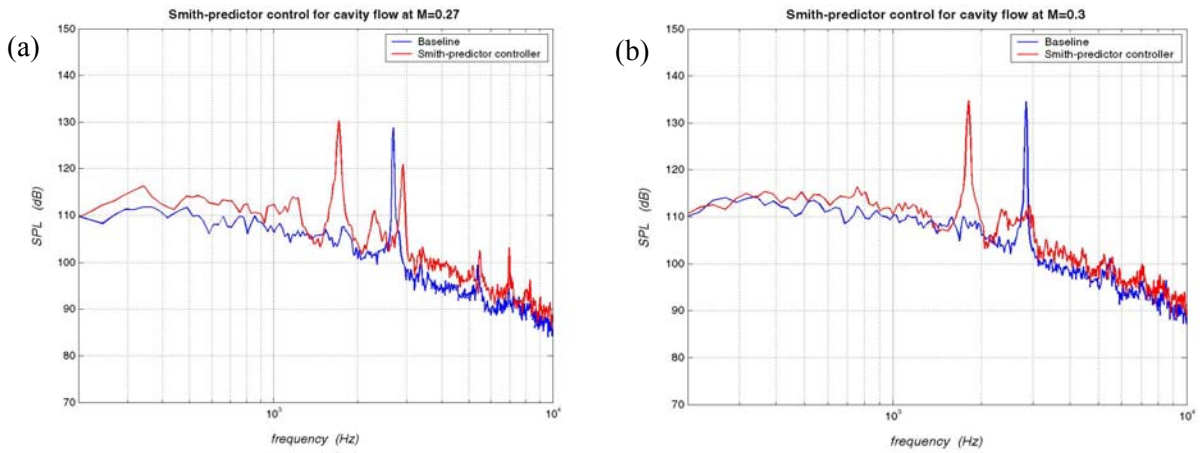


Figure 4.4 Effect of Smith predictor-based control on Mach 0.27 flow (a) and on Mach 0.3 flow (b); upper (thin) line is the baseline flow SPL spectrum and lower (thick) line is the controlled flow.

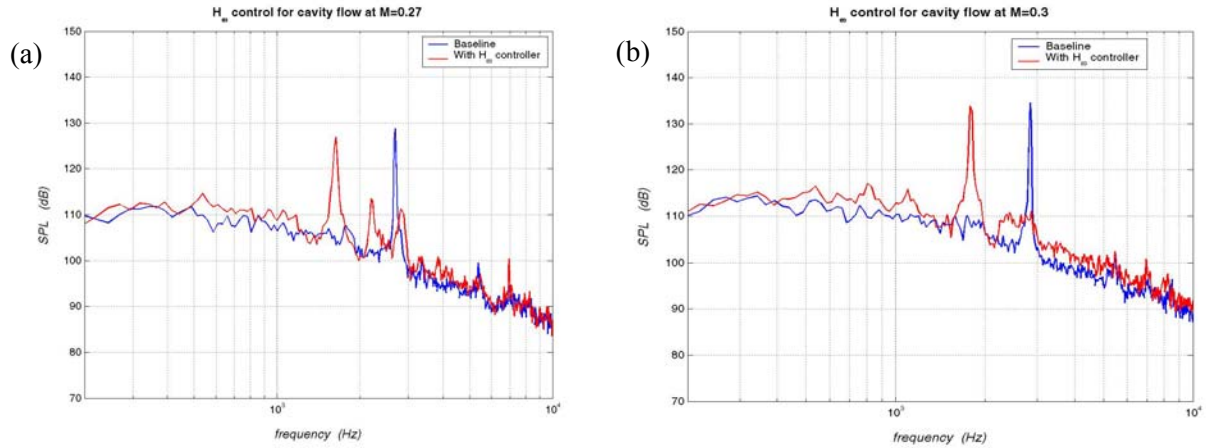


Figure 4.5 Effect of H^∞ control on Mach 0.27 flow (a) and on Mach 0.3 flow (b); upper (thin) line is the baseline flow SPL spectrum and lower (thick) line is the controlled flow.

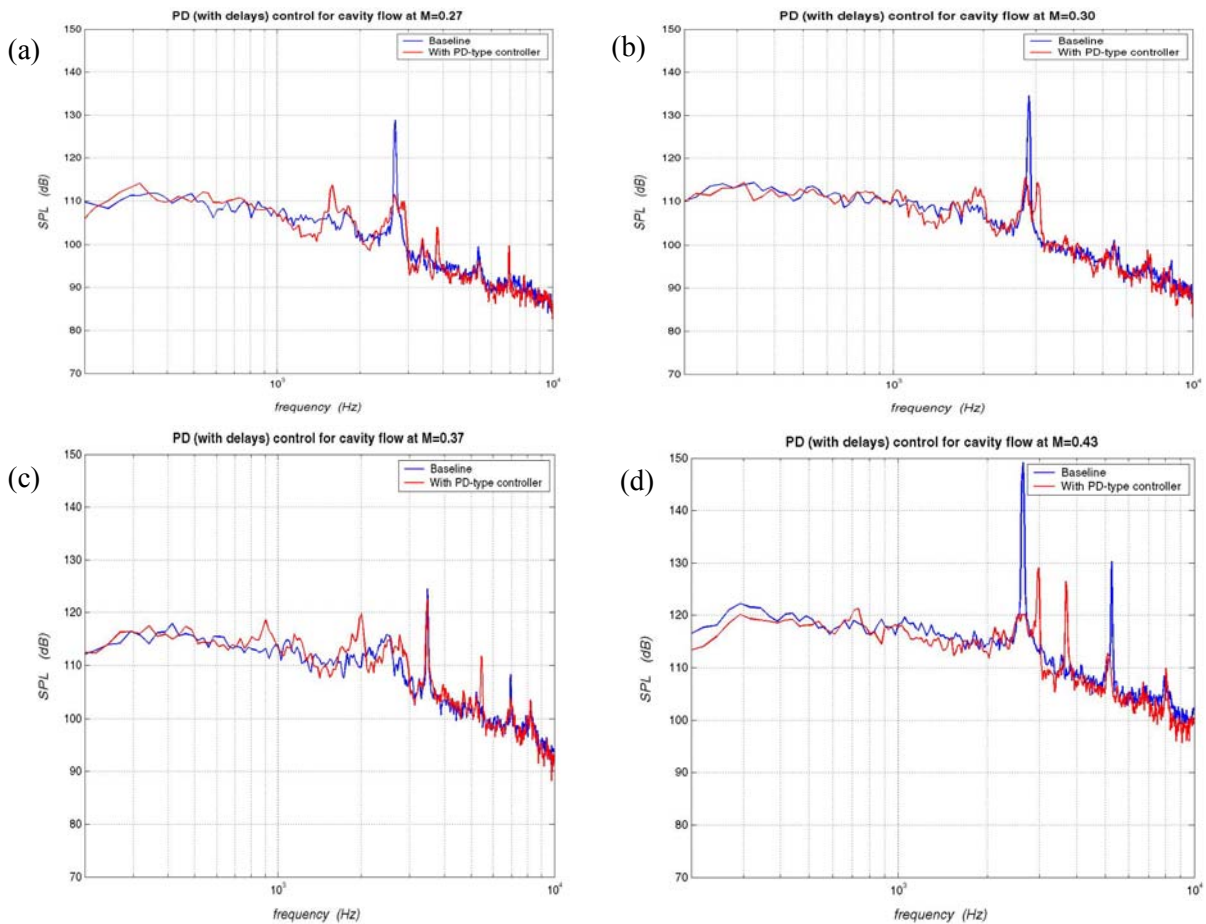


Figure 4.6 Effect of PD-like (effectively P-P) control with time delay of $260 \mu s$ on the derivative term (zero placement at 1923 Hz); Mach 0.27 flow (a); Mach 0.3 flow (b); Mach 0.37 flow (c); Mach 0.43 flow (d). Upper (thin) line is the baseline flow SPL spectrum; lower (thick) line is the controlled flow.

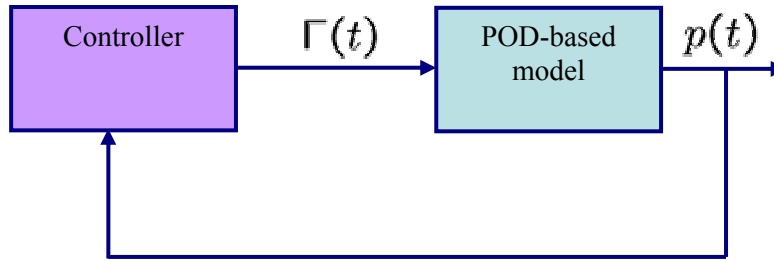


Figure 5.1 Simulink implementation of the nonlinear model and the controller.

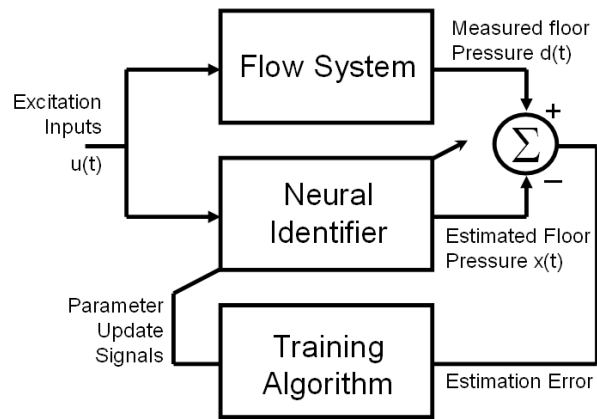


Figure 5.2 Neural Network based identification

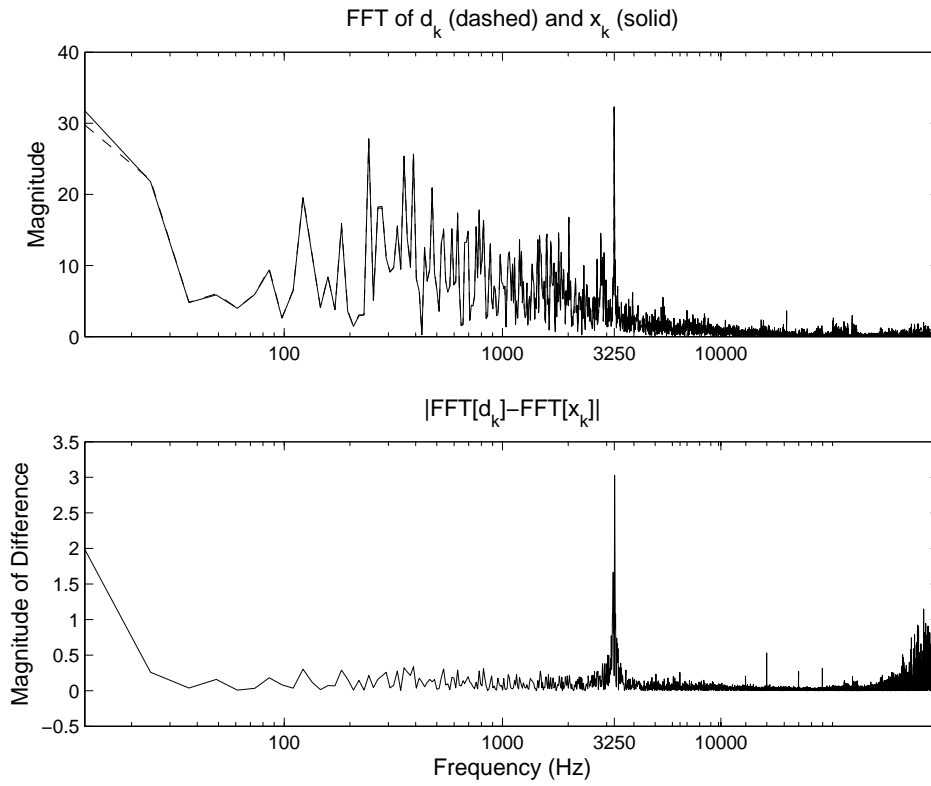


Figure 5.3 Comparison of the frequency contents of the measured and estimated pressure output signals.